Aeroelastic Analysis of Rotor Blades Using Nonlinear Fluid/Structure Coupling *

H. Murty, C. Bottasso, M. Dindar, M. Shephard, O. Bauchau
Rensselaer Polytechnic Institute
Troy, NY

Abstract

Aeroelastic stability analysis of rotorcraft requires accurate loads and structural dynamic analysis. Research and develoment efforts indicate that computational fluid dynamics (CFD) codes can provide more accurate loads prediction. In this paper, aeroelastic analysis of rotor blades was carried out by computational coupling between a computational fluid dynamics (CFD) program and a computational structural dynamics (CSD) program. Time response aeroelastic blade deformation was used to obtain damping information.

Introduction

The investigation of aeroelastic stability characteristics of rotorcraft blades involves accurate determinaton of the aerodynamic loads and moments. Traditionally such aerodynamic computations have been carried out using quasi-steady aerodynamics or panel methods. For many applications such models may be adequate. However, effects of transonic tip Mach number and accurate wake prediction are not included. These effects are important at large angles of collective pitch or high rotational speeds relative to the specific blade geometry. Since helicopter blades are usually torsionally soft, significant deformations of the blade may occur and the aerodynamic computational fluid dynamics (CFD) code must be able to accomodate large displacements accurately. Under such conditions, panel methods or linear aerodynamic theory, which use flat plate lift curve slopes, will not accurately predict the stability conditions.

Kwon et al [1] and Smith and Hodges [2] have analyzed a rotor blade from the Integrated Technology Rotor Assessment Workshop [13] held at NASA Ames Research Center in 1988. Kwon et al carried out an aerodynamic analysis using a panel method and then used that load information in a structural dynamics code based on modal analysis. Equilibrium deflections of the blade in hover were obtained. In addition, a dynamic analysis was carried out to obtain damping and frequency of the system. Smith used an Euler/Navier-Stokes code based on finite differences on a structured mesh and obtained equilibrium deflections for the same test case. Considerable differences were observed for the results of Smith and Kwon for certain conditions. The differences were attributed to the aerodynamic model used.

In this study, a parallel, adaptive, finite element CFD code was used to solve the Euler equations. An implicit time discontinuous, Galerkin, least squares method [3] was developed and validated [4] for flow over a rotary wing in hover. The loads obtained for this CFD code based on finite elements on an unstructured mesh were used and coupled with a multi-body, structural dynamics code. The CFD code is unconditionally stable as measured in its natural entropy norm [3]. In addition, the structural dynamics code, DYMORE, is unconditionally stable using the energy decay argument, as shown in [5]. These coupled computational codes

*Submitted to the American Helicopter Society, Annual Forum Conference, 1996.

were used to carry out comparisons with the test case used by Kwon et al and Smith. For small angles of collective pitch, agreement between the different methods is good. However, the benefit of the more exact Euler code is apparent at larger values of collective pitch angle for which panel method predictions could not be adequate, especially in supercritical flowfields.

In this study, the basic coupling scheme between a space-time, finite element CFD code and multibody dynamics CSD code is investigated for a practical rotor blade aeroelastic analysis. Such studies are important in assessing the computational capabilities to carry out adequate rotorcraft aeroelasticity. The results of this study and continuing research enable us to apply these developments to practical rotorcraft applications.

Finite Element Formulation

A finite element formulation is developed for the solution of the Navier-Stokes/Euler equations,

$$\operatorname{div} \boldsymbol{F} + \mathcal{F} = 0 \qquad (1)$$

with well posed initial and boundary conditions. In equation (1), div is the divergence operator in $n_{sd}+1$ space–time dimensions, where n_{sd} is the number of space dimensions, while $\boldsymbol{F} = (\boldsymbol{U}, \boldsymbol{F}_i - \boldsymbol{F}_i^d)$, where $\boldsymbol{U} = \rho(1, u_1, u_2, u_3, e)$ are the conservative variables, $\boldsymbol{F}_i = \rho\, u_i(1, u_1, u_2, u_3, e) + p\,(0, \delta_{1i}, \delta_{2i}, \delta_{3i}, u_i)$ is the Euler flux, $\boldsymbol{F}_i^d = (0, \tau_{1i}, \tau_{2i}, \tau_{3i}, \tau_{ij}u_j) + (0, 0, 0, 0, -q_i)$ is the diffusive flux, and $\mathcal{F} = \rho\,(0, b_1, b_2, b_3, b_i u_i + r)$ is the source vector. In the previous expressions, ρ is the density, $\boldsymbol{u} = (u_1, u_2, u_3)^T$ is the velocity vector, e is the total energy, p is the pressure, δ_{ij} is the Kronecker delta, $\boldsymbol{\tau} = [\tau_{ij}]$ is the viscous stress tensor, $\boldsymbol{q} = (q_1, q_2, q_3)^T$ is the heat–flux vector, $\boldsymbol{b} = (b_1, b_2, b_3)^T$ is the body force vector per unit mass and r is the heat supply per unit mass.

The Time–Discontinuous Galerkin Least–Squares (TDG/LS) finite element method is used in this investigation [3]. This method is developed starting from the symmetric form of the Navier–Stokes/Euler equations expressed in terms of entropy variables and it is based upon the simultaneous discretization of the space–time computational domain. A least–squares operator and a discontinuity capturing term are added to the formulation for improving stability without sacrificing accuracy. The TDG/LS finite element method takes the form

$$\begin{aligned}
&\int_{Q_n} \left(-\boldsymbol{W}^h_{,t} \cdot \boldsymbol{F}(\boldsymbol{V}^h) + \boldsymbol{W}^h \cdot \tilde{\boldsymbol{C}} \boldsymbol{V}^h\right) \mathrm{d}Q \\
&+ \int_{\Omega(t_{n+1})} \boldsymbol{W}^{h^-} \cdot \boldsymbol{U}(\boldsymbol{V}^{h^-})\, \mathrm{d}\Omega - \\
&\int_{\Omega(t_n)} \boldsymbol{W}^{h^+} \cdot \boldsymbol{U}(\boldsymbol{V}^{h^-})\, \mathrm{d}\Omega \\
&+ \int_{P_n} \boldsymbol{W}^h \boldsymbol{F} \cdot \mathrm{d}\boldsymbol{P} \\
&+ \sum_{e=1}^{(n_{el})_n} \int_{Q_n^e} \left(\mathcal{L}\boldsymbol{W}^h\right) \cdot \tau \left(\mathcal{L}\boldsymbol{V}^h\right) \mathrm{d}Q \\
&+ \sum_{e=1}^{(n_{el})_n} \int_{Q_n^e} \nu^h \hat{\nabla}_\xi \boldsymbol{W}^h \cdot \operatorname{diag}[\tilde{\boldsymbol{A}}_0] \hat{\nabla}_\xi \boldsymbol{V}^h \, \mathrm{d}Q = 0. \qquad (2)
\end{aligned}$$

Integration is performed over the space–time slab Q_n, the evolving spatial domain $\Omega(t)$ of boundary $\Gamma(t)$ and the surface P_n described by $\Gamma(t)$ as it traverses the time interval $I_n =]t_n, t_{n+1}[$. $\boldsymbol{W}^h$ and $\boldsymbol{V}^h$ are suitable spaces for test and trial functions, while τ and ν^h are appropriate stabilization parameters. Additional details on the TDG/LS finite element formulation are given in [3].

Two different three dimensional space–time finite elements were implemented. The first is based on a constant in time interpolation, has low order of time accuracy but good stability properties, and is well suited for solving steady problems. The second makes use of linear–in–time basis functions, exhibits a higher order temporal accuracy, and is well suited for addressing unsteady problems. As pointed out by Tezduyar et al. [6], this latter element naturally allows direct treatment of moving boundary problems. In fact the motion of boundaries or interfaces is automatically included in the Jacobian that relates the physical space–time coordinates with the local finite element space–time coordinates. The only difficulty in this case arises in three dimensional applications when one has to compute the space–time boundary integral. This term appears as a consequence of the integration by parts performed in the four dimensional domain,

and represents the flux that traverses the three dimensional space–time boundary. This problem can be solved using the concept of differential forms and the General Stokes' Theorem (see for example Corwin and Szczarba [7]).

Discretization of the weak form implied by the TDG/LS method leads to a non–linear discrete problem, which is solved iteratively using a quasi–Newton approach. At each Newton iteration, a non–symmetric linear system of equations is solved using the GMRES algorithm [8].

Structural Dynamics Model

The structural model of the helicopter blade incorporates flap bending, chordwise bending and torsion of a slender beam with constant spanwise mass and stiffness properties. The blade is rotating at a constant angular speed about an axis fixed in space. The computational structural dynamics (CSD) code is capable of modeling general nonlinear, elastic, multi-body systems using the finite element method [5] [9] [10]. The formulation uses Cartesian coordinates to represent the position of each elastic body with respect to a single inertial frame. Lagrange multipliers are used to enforce kinematic constraints among the various bodies of the system. The equations of motion are discretized so that they imply an energy decay inequality for the elastic components of the sytem, while the forces of constraint are discretized so that the work they perform vanishes exactly. It can be proved that this solution system is unconditionally stable using the energy decay argument, as shown in [5]. In this preliminary study, the rotor blade is modelled as a cantilever beam, with distributed torsional rigidity. This model is the one used in the Integrated Technology Assessment Workshop. However, more complicated connections are possible between the hub and the blade.

Coupling Methodology

The coupling conditions between the CFD and CSD code affect the resulting aeroelastic stability predictions. The analysis could be carried out using fully coupled or staggered analysis procedures as defined by Farhat [11]. It is clear that fully coupled procedures are computationally intensive. Staggered strategies require coupling of the CFD and CSD codes at intermediate time steps. In this initial study, the basic coupling scheme was used for the computations in hover as described in the following. The converged CFD computations of loads were used in the CFD computations in order to determine the deflected blade geometry. The general dynamic aeroelastic procedure consists of first determining a steady flow field and then perturbing the flow field by inducing a small displacement. The general fluid/structure coupling algorithm for the time response is then analysed as illustrated by the flowchart in Figure 1. The coupling process must also account for the dimensional difference between the mathematical models used in the current CFD and CSD procedures as shown in Figure 2. The pressure load from the 3-D CFD analysis is transferred to the 1-D beam of the CSD analysis by the appropriate integrations of the blade surface pressure at the CSD beam stations. The deformations calculated in the CSD analysis are reflected in the CFD analysis by applying the beam displacements and rotations to rigid cross sections at the beam stations which are then used to define a new blade geometry by lofting a surface through those cross sections.

Coupling Results in Equilibrium

Aeroelastic computations were carried out for a rotating blade in hover [12]. The geometry of the experimental model rotor hub design is shown in Figure 3. This model differs from the simplified model used in the Integrated Technology Rotor(ITR) Assessment Workshop [13] which is a cantilever beam with a distributed value of torsional rigidity. The ITR model was used in the present study. A converged CFD computation was carried out at 4 degree collective pitch angle, using 200,000 elements for two rotor blades. The pressure distributions in hover at the midspan location is shown in Figure 4. Spanwise lift, drag and moment coefficient, shown in Figure 5, were computed and input to the struc-

tural dynamics code. Equilibrium deflections in torsion, flap and lead-lag were obtained and are shown in Figure 6. A comparison of results with those of other investigators is given in the accompanying table:

	Flap /radius	Lead-Lag /radius	Torsion degrees
Kwon (panel method)	0.015	0.002	0.5
Smith (Euler)	0.012	0.0002	0.4
Current Investigation	0.012	0.0001	0.1

The flap deflections seem to be in good agreement for this case. For this subcritical flow case, the lift coefficient should be well predicted by panel methods. Since flap deflection is primarily associated with the lift force, assuming that coupling contributions are minimal, those values are similar for all three investigations.

The pressure drag forces predicted by panel methods will differ from that computed by the Euler equations. This inviscid drag contribution comes from the curvature of the airfoil section which the panel method approximates with only 200 panels on the blade surface compared to approximately 500 for both investigations using Euler equations. This force, along with the coupling contribution from other modes, is primarily responsible for the lead-lag deflection. Hence, Kwon's results differ from the other two investigations primarily owing to this difference in aerodynamic modelling.

The torsion of the system is dependent on the pitch flexure mechanism used in the model. Both Kwon's and Smith's use equivalent torsional springs to link the hub with the blade, whereas the current study used the ITR model which treated the blade as a cantilever beam with distributed torsional rigidity. This difference in torsional modelling is primarily responsible for the difference in torsional deflections, assuming minimal coupling effects.

Dynamic Aeroelastic Coupling

Previous investigations in this area of research have attempted some improvements to the aerodynamic model used in the analysis using basic coupling schemes. Chopra et al [14] carried out an investigation to predict structural and aerodynamic loads on the rotor blade of a SA 349/2 Gazelle helicopter. The aerodynamic analysis was carried out using a small disturbance potential flow code. The angle of attack distribution from the inflow is determined and applied as a boundary condition to the fluid flow solver from which the pressure distribution on the blades was determined. This type of coupling is usually termed loose coupling and is the predominant coupling scheme used in most CFD/CSD code interactions. A subsequent investigation by Torok and Chopra [15] also followed along similar lines by including nonlinear effects and the comparison to flight test data in forward flight was good for an isolated, soft inplane hingeless rotor with discrete flap and lead-lag flexures and relatively rigid blades. The coupling methodology solved the system of equations iteratively using a modified Newton method, satisfying blade and trim equilibrium equations. The Leishman and Beddoes [19] aerodynamic state space model was used in order to solve the complete system. The same aerodynamic model was also used by Murty [20] in order to solve the system of coupled equations using hard coupling. Kwon et al [1] used a three dimensional panel method algorithm using potential flow theory. However, the aerodynamic model was incompressible and therefore, only effective for low angles of attack. Consequently, the dynamic analysis did not provide adequate results in comparison with experimental data for the damping for large angles of attack. Kwon also used the basic coupling scheme of consecutive flow and structural dynamic solutions. Subsequent investigations by Smith et al [2] were limited to equilibrium deflections of the rotor blade. The aerodynamic analysis was carried out by an Euler/Navier-Stokes code and a prescribed wake model was included. The condition at which equilibrium deflections would be computed by the structural dynamics solver was varied.

More recently, Farhat [21] carried out an investigation into coupling of nonlinear, transient aeroelastic problems. This basic scheme starts with the converged flow solution in hover for the rotor blades. The system is then perturbed in the mode of interest and the flow field solution is then obtained at these new conditions. It is at this stage that internal Newton iterations are used to obtain a converged fluid flow solution at this time step. The pressure load from this solution is used in determining the structural dynamics solution. Subsequently the deformation information is used to modify the fluid flow solution appropriately. The extensive numerical investigation of Farhat determined that this scheme is stable for time steps within the fluid flow solver stability. This information was used in this study and found to give results which were numerically stable with the appropriate time step.

The CSD code determined the displacements along discrete spanwise locations. This information is then used to modify the model geometry and build a new rotor blade model. A mesh motion procedure is used to locally update the mesh close to the moving surface to account for the geometry changes. The completion of this procedure, provides a new model and mesh to the CFD solver which produces a new flow solution in turn. The mesh motion procedure of Batina [16] was used.

To obtain the dynamic aeroelastic response of the rotor blade, a perturbation in lead-lag was initially applied and the aeroelastic response of the blade in time was observed. After 100 time steps (which corresponds to 17 degrees of rotational motion), the torsional, flap-lag and torsional-lag displacements were examined (Figures 7, 8 and 9). The time response of the lead-lag mode of interest, is shown in Figure 10. Spanwise distributions of lead-lag and flap displacements are shown in Figure 11. The mode shapes can be discerned from this plot. FFT can be accurately used to determine the damping of the response. In this study, the damping obtained for this model was -2.100 rad/s. The experimental value obtained by Sharpe [12] was -2.172 rad/s giving a 3.31 percent difference between the computational value and experimental value.

Concluding Remarks

An aeroelastic analysis was carried out for the specific case of a rotor in hover. Equilibrium deflections in hover were obtained in flap, lead-lag and torsion modes. These results were compared with those obtained by previous investigators. Differences observed could be attributed to specific differences in the aerodynamic and structural modelling used in the individual investigations. A dynamic aeroelastic analysis was carried out using the linear-in-time finite element formulation for the fluid flow coupled with a structural dynamic analysis. Such an analysis can be used to increase the accuracy of aeroelastic stability damping computations for rotor blades

Acknowledgements

The authors would like to acknowledge the Army Research Office for funding this research through the ARO Rotorcraft Technology Center at Rensselaer Polytechnic Institute (DAAH04–93–G–0003, G. Anderson project monitor).

References

[1] Kwon, O. J., Hodges, D. H., Sankar, L. N., "Stability of Hingeless Rotors in Hover using Three-Dimensional Unsteady Aerodynamics", *Journal of the American Helicopter Society*, pages 21-31 April 1991.

[2] Smith, M. J. and Hodges, D. H., "Development of an Aeroelastic Method for Hovering Rotors with Euler/Navier Stokes Aerodynamics", American Helicopter Society 51st Annual Forum, Fort Worth, TX, May 9-11, 1995.

[3] Shakib, F., Hughes, T. J. R. and Zohan, J., "A New Finite Element Formulation for Computational Fluid Dynamics: X. The Compressible Euler and Navier Stokes Equations", *Comp. Meth. Appl. Mech. Eng.*, 89:141-219, 1991.

[4] Bottasso, C. L., Shephard, M. S., "A Parallel Adaptive Finite Element Euler Flow Solver for

Rotary Wing Aerodynamics", AIAA 12th Computational Fluid Dynamics Conference, San Diego, June 19-22, 1995(to appear in AIAA Journal).

[5] Bauchau, O. A., Damilano G., and Theron N.J., Numerical "Integration of Nonlinear Elastic Multi-body Systems", accepted for publication in the *International Journal of Numerical Methods in Engineering*, 1995.

[6] Tezduyar, T.E., Behr, M., Mittal, S. and Liou J., "A New Strategy for Finite Element Computations Involving Moving Boundaries and Interfaces – The Deforming–Spatial–Domain/Space–Time Procedure: I. The Concept and the Preliminary Tests", *Comp. Meth. Appl. Mech. Eng.*, 94:353–371, 1992.

[7] Corwin, L.J. and Szczarba, R.H., *Calculus in Vector Spaces*, Marcel Dekker Inc., 1979.

[8] Saad, Y. and Schultz, M., "GMRES: A Generalized Minimum Residual Algorithm for Solving Nonsymmetric Linear Systems", *SIAM J. Sc. Stat. Comp.*, 7:856–869, 1986.

[9] Bauchau, O. A., Lee, M., Theron, N. J., "Energy Decaying Scheme with Adaptive Time Step Methodology for Nonlinear Beam Models", 36th AIAA/ASME/ASCE/AHS/ASC Structures, Structural Dynamics, and Materials Conference, April 10-13, 1995, New Orleans, LA.

[10] Bauchau O.A., and Theron N.J., "Energy Decaying Schemes for Nonlinear Beam Models", accepted for publication in *Computer Methods in Applied Mechanics and Engineering*, 1995.

[11] Farhat, C., Lesoinne, M. and Chen, P. S., "Parallel Heterogeneous Algorithms for the Solution of Three-Dimensional Transient Coupled Aeroelastic Problems", 36th AIAA/ASME/ASCE/AHS/ASC Structures, Structural Dynamics, and Materials Conference, April 10-13, 1995, New Orleans, LA.

[12] Sharpe, D. L., "An Experimental Investigation of the Flap-Lag-Torsion Aeroelastic Stability of a Small-Scale Hingeless Helicopter Rotor in Hover", NASA TP 2546, AVSCOM Technical Report 85-A-9, 1986.

[13] Bousman, W. G., "Rotorcraft Aeromechanical Stability – Methodology Assessment: Phase 2 Workshop", NASA Technical Memorandum 102272, March 1990.

[14] K. C. Kim, A. Desopper and I. Chopra, "Blade Response Calculations Using Three Dimensional Aerodynamic Modeling ", *Journal of the American Helicopter Society*, pages 68-77 January 1991.

[15] M. S. Torok and I. Chopra, "Hingeless Rotor Aeroelastic Stability Analysis with Refined Aerodynamic Modeling", *Journal of the American Helicopter Society*, pages 48-56 October 1991.

[16] B. A. Robinson, J. T. Batina and H. T. Y. Yang, "Aeroelastic Analysis of Wings Using the Euler Equations with a Deforming Mesh", *Journal of Aircraft*, pages 781-788 November 1991.

[17] O. O. Bendiksen, "A New Approach to Computational Aeroelasticity", 32nd AIAA/ASME/ASCE/AHS/ASC Structures, Structural Dynamics, and Materials Conference, April 8-10, 1991, Baltimore, MD.

[18] H. S. Murty and G. W. Johnston, "Nonlinear Aspects of Transonic Aeroelasticity", *Canadian Aeronautics and Space Journal*, Volume 39, Number 2, Pages 78-84, 1993 (also University of Toronto Institute for Aerospace Studies (UTIAS) Report No. 345, January 1992).

[19] J. G. Leishman, "Validation of Approximate Indicial Aerodynamic Functions for Two-Dimensional Subsonic Flow", *Journal of Aircraft*, Volume 25, (10), October 1988.

[20] H. S. Murty, "Aeroelastic Stability Analysis of an Airfoil with Structural Nonlinearities Using a State Space Unsteady Aerodynamics Model", 36nd AIAA/ASME/ASCE/AHS/ASC Structures, Structural Dynamics, and Materials Conference, April 10-13, 1995, New Orleans, LA.

[21] C. Farhat, "High Performance Simulation of Coupled Nonlinear, Transient Aeroelastic Problems", in Parallel Computing in CFD, volume R-807, pages 6.1-6.49, AGARD, Neuilly-Sur-Seine, France, 1995.

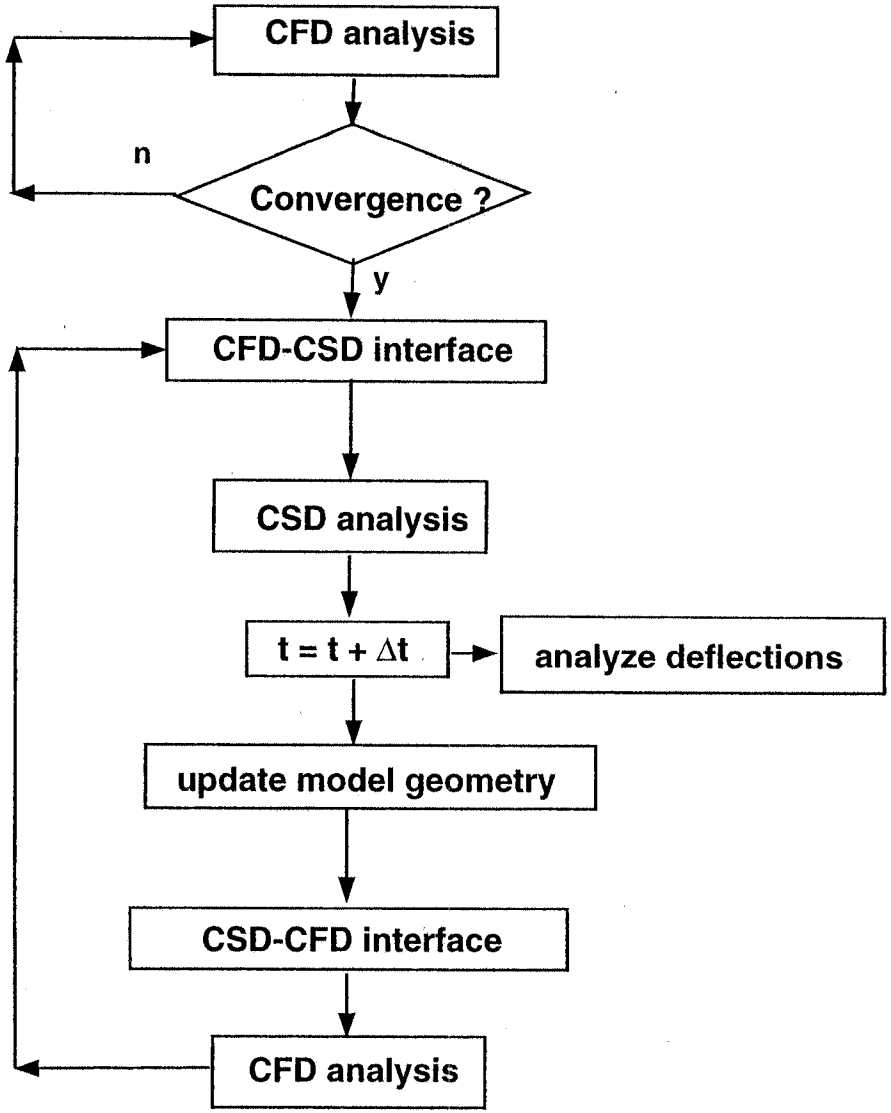

Fig. 1 Flowchart for fluid/structure basic coupling scheme

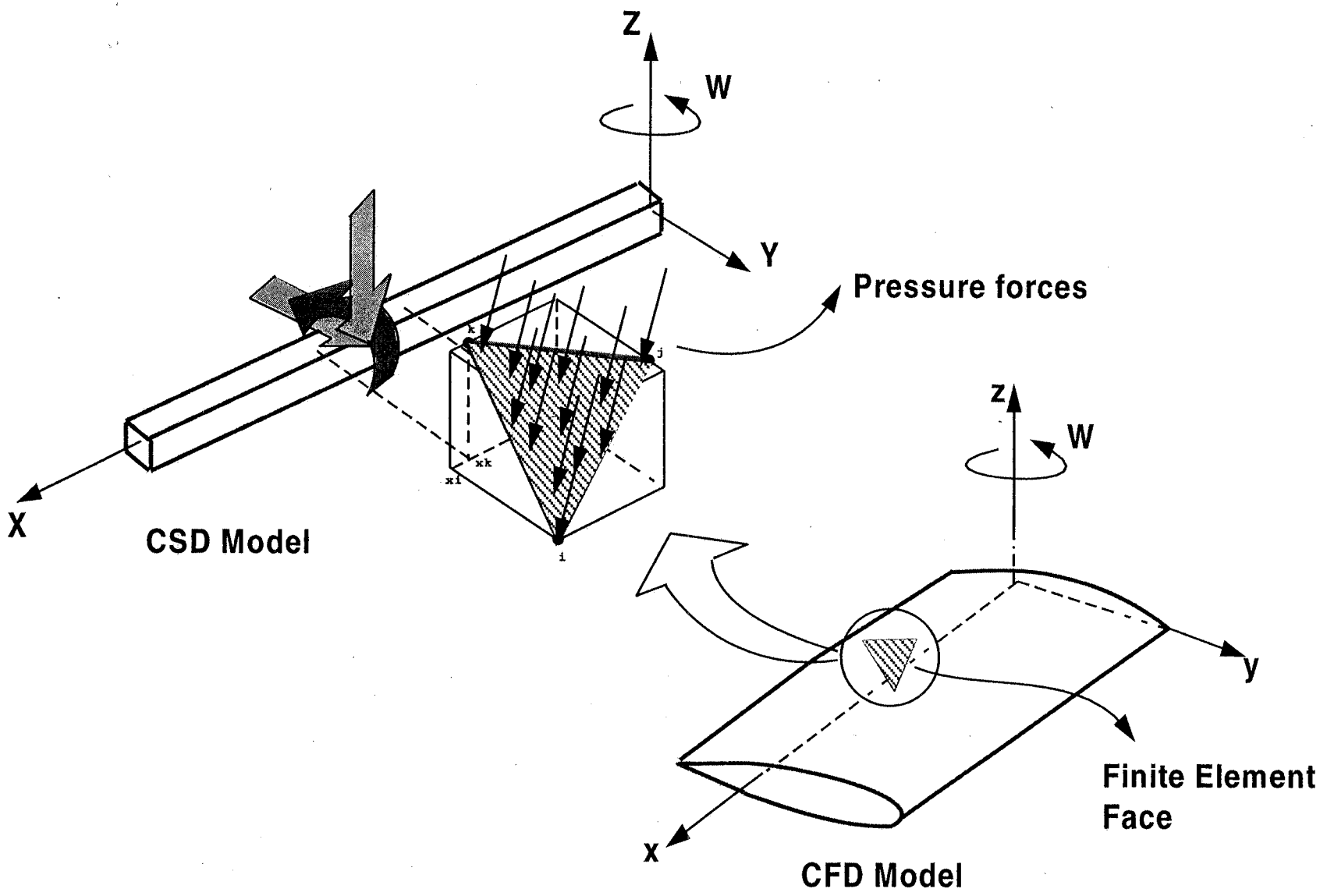

Figure 2 Mapping 3-d pressure distribution from CFD code to 1-d CSD code

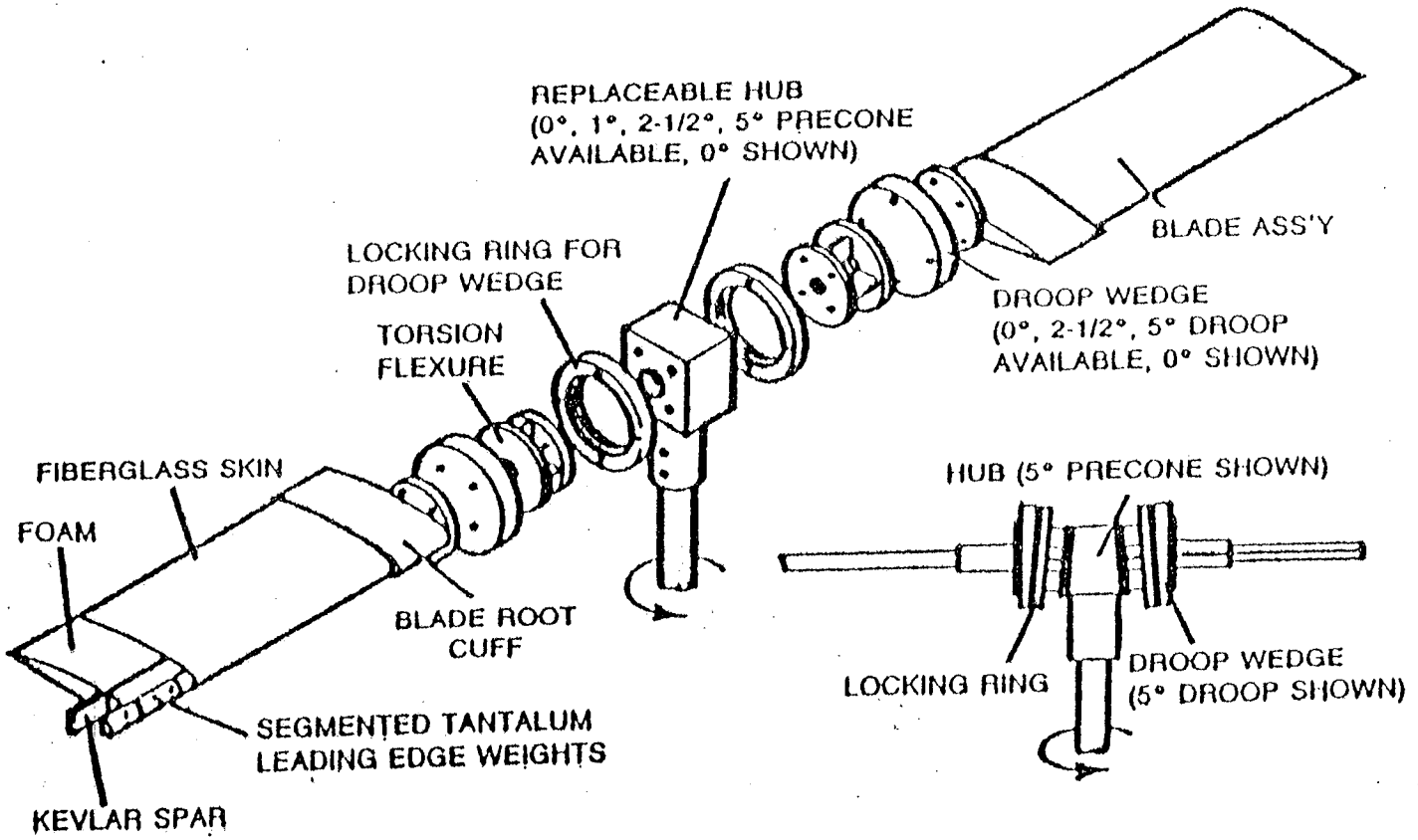

Figure 3 Experimental model rotor hub

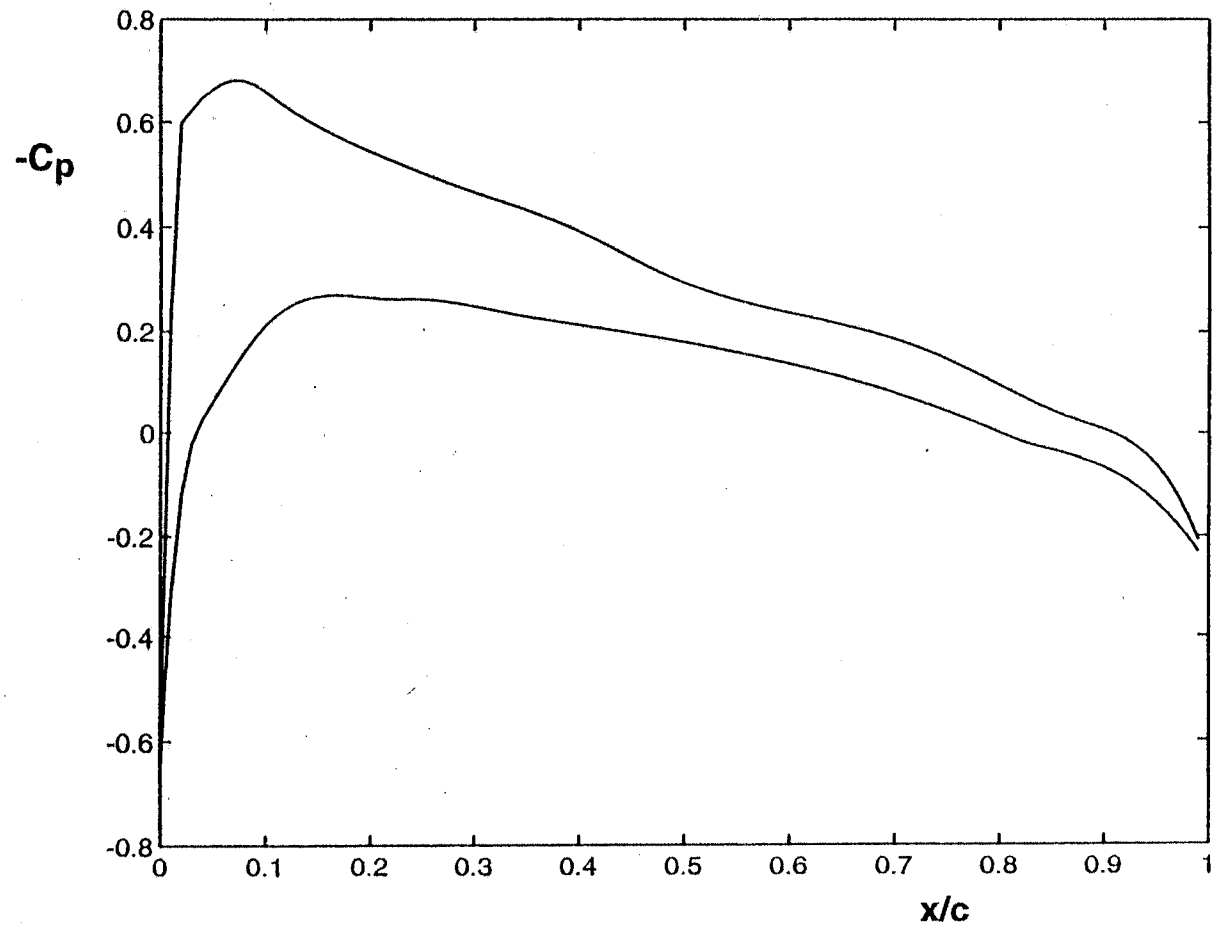

Fig. 4 Pressure Coefficient over mid-span section of rotor blade in hover

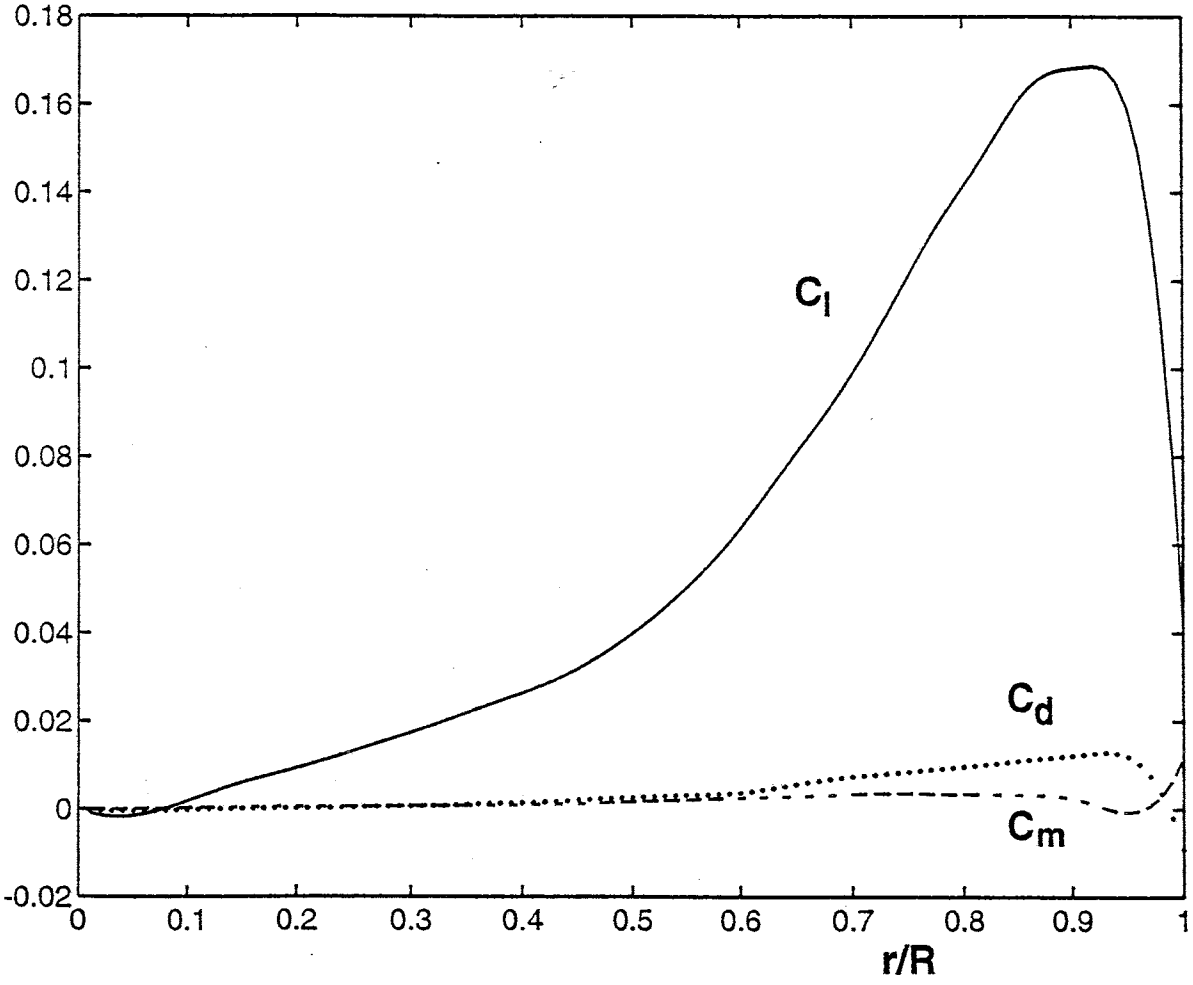

Fig. 5 Coefficients of lift, drag and moment for rotor blade in hover (M_{tip}= 0.3, pitch angle = 4 deg.)

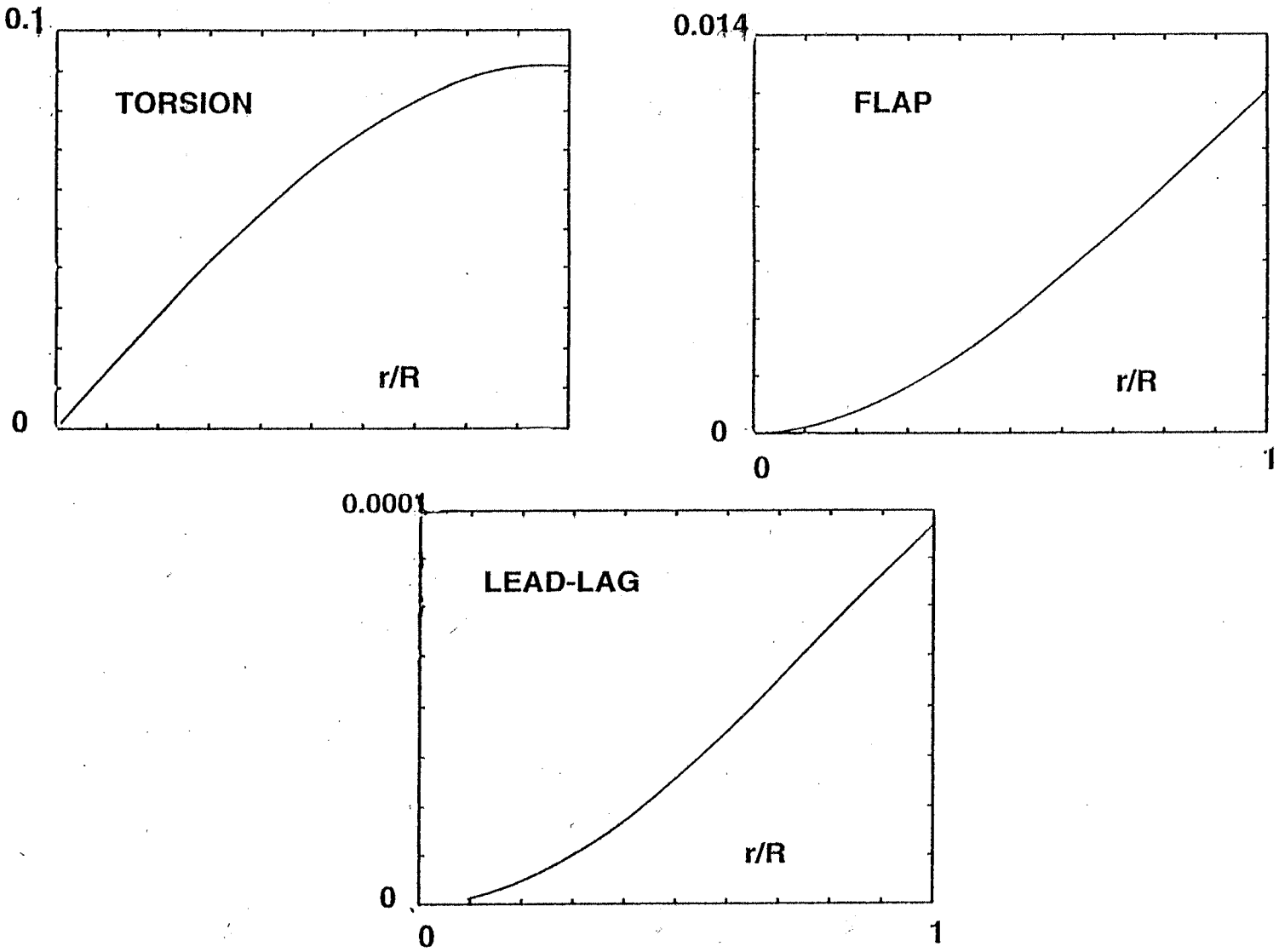

Fig. 6 Equilibrium deflections of a rotor blade in hover

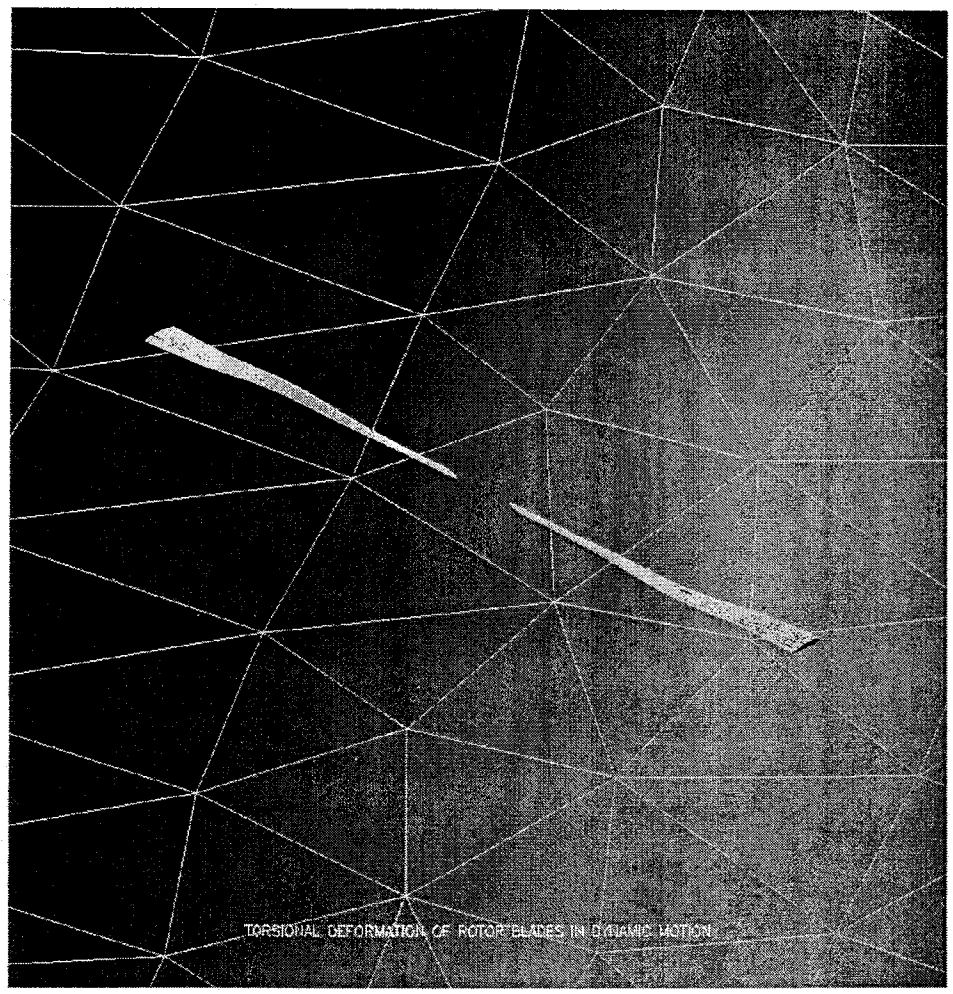

Figure 7 Aeroelastic deformation of Sharpe rotor blades magnified by a factor of 100,000.

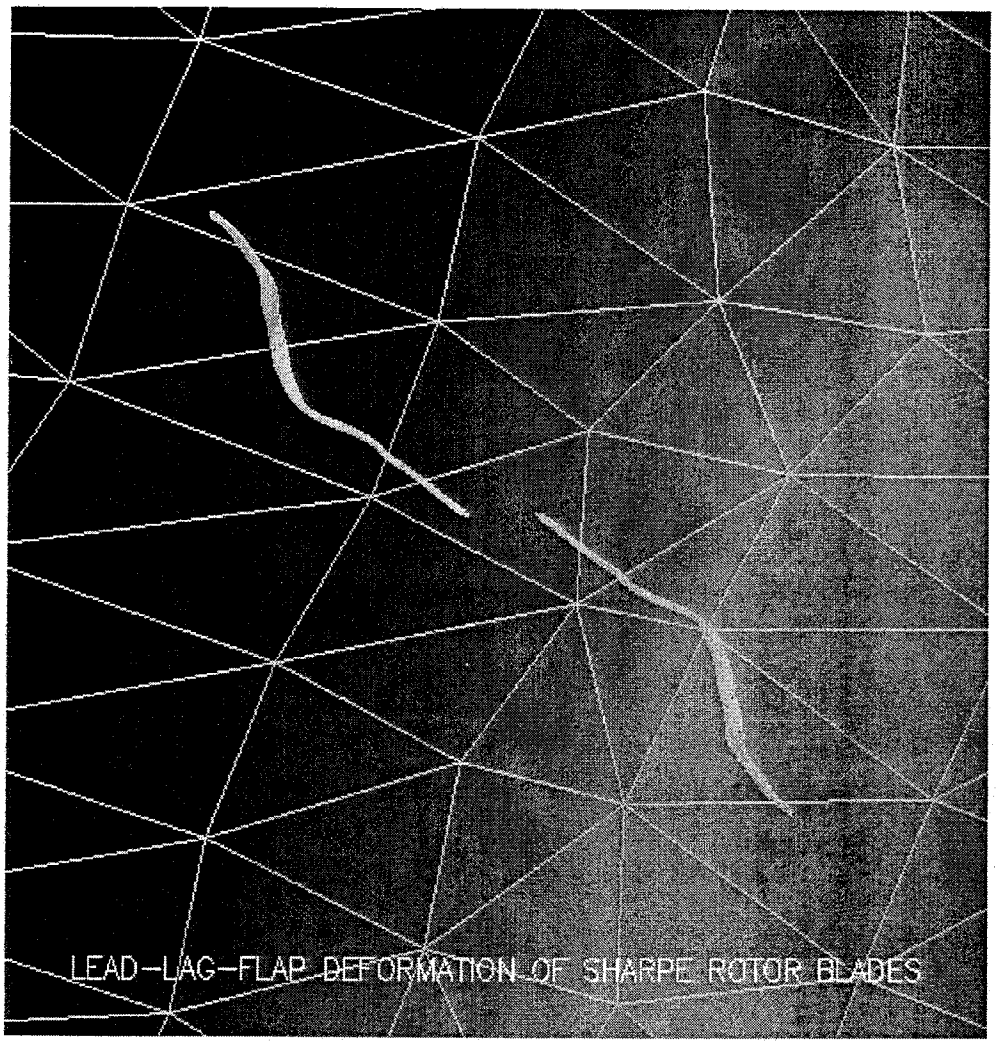

Figure 8 Aeroelastic deformation of Sharpe rotor blades magnified by a factor of 100,000(deformation in lead-lag-flap).

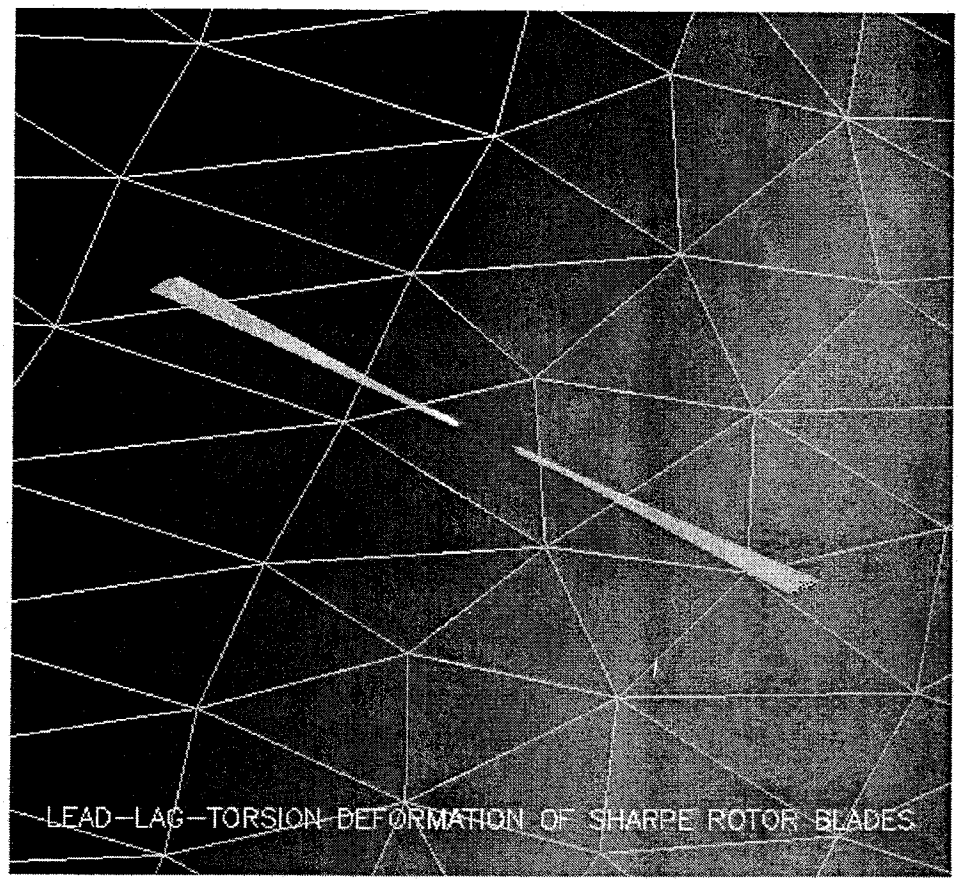

Figure 9 Aeroelastic deformation of Sharpe rotor blades magnified by a factor of 100,000(deformation in lead-lag-torsion).

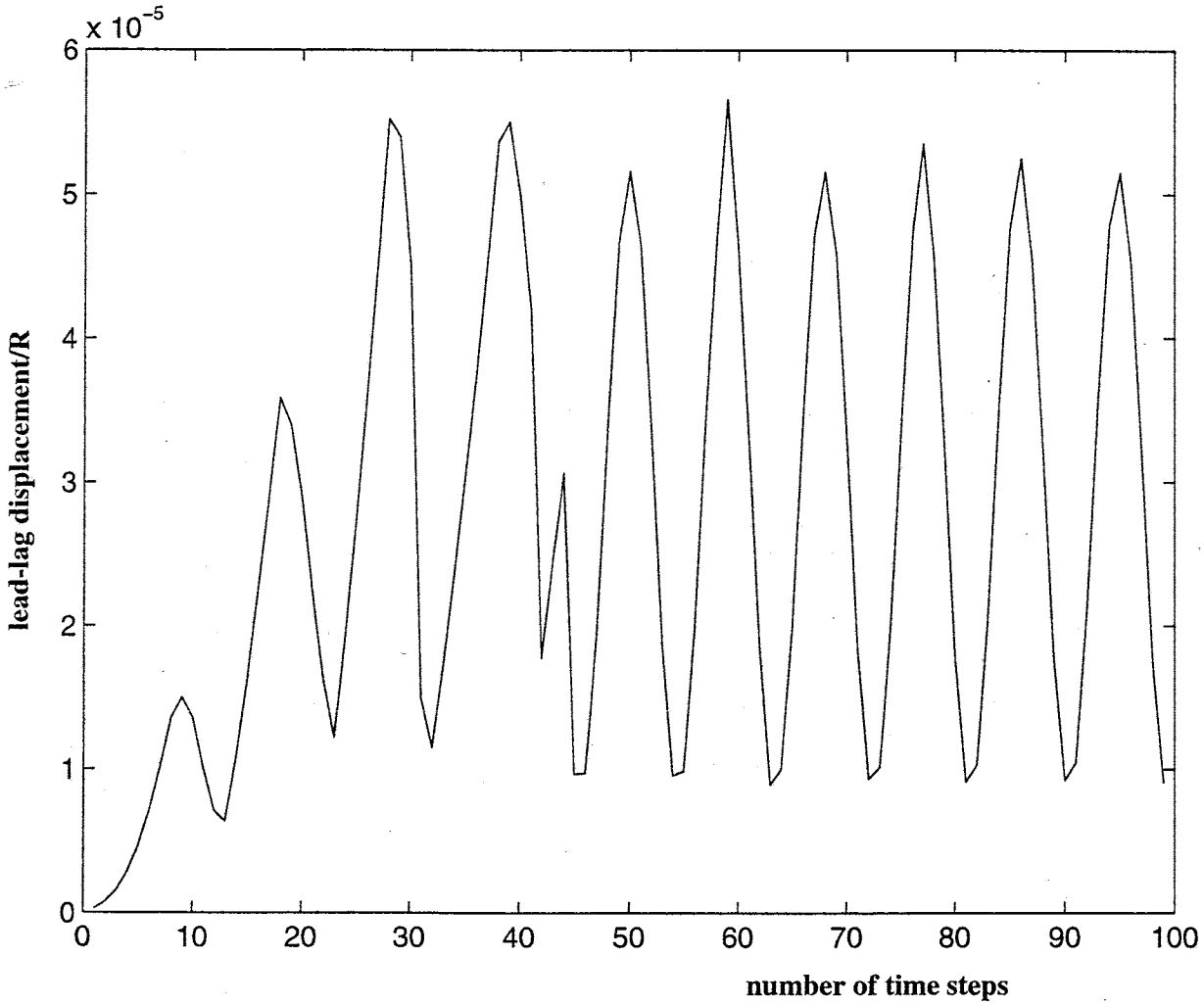

Figure 10 Aeroelastic time response of Sharpe rotor blade in hover (M(tip) = 0.296 collective pitch = 4 degrees)

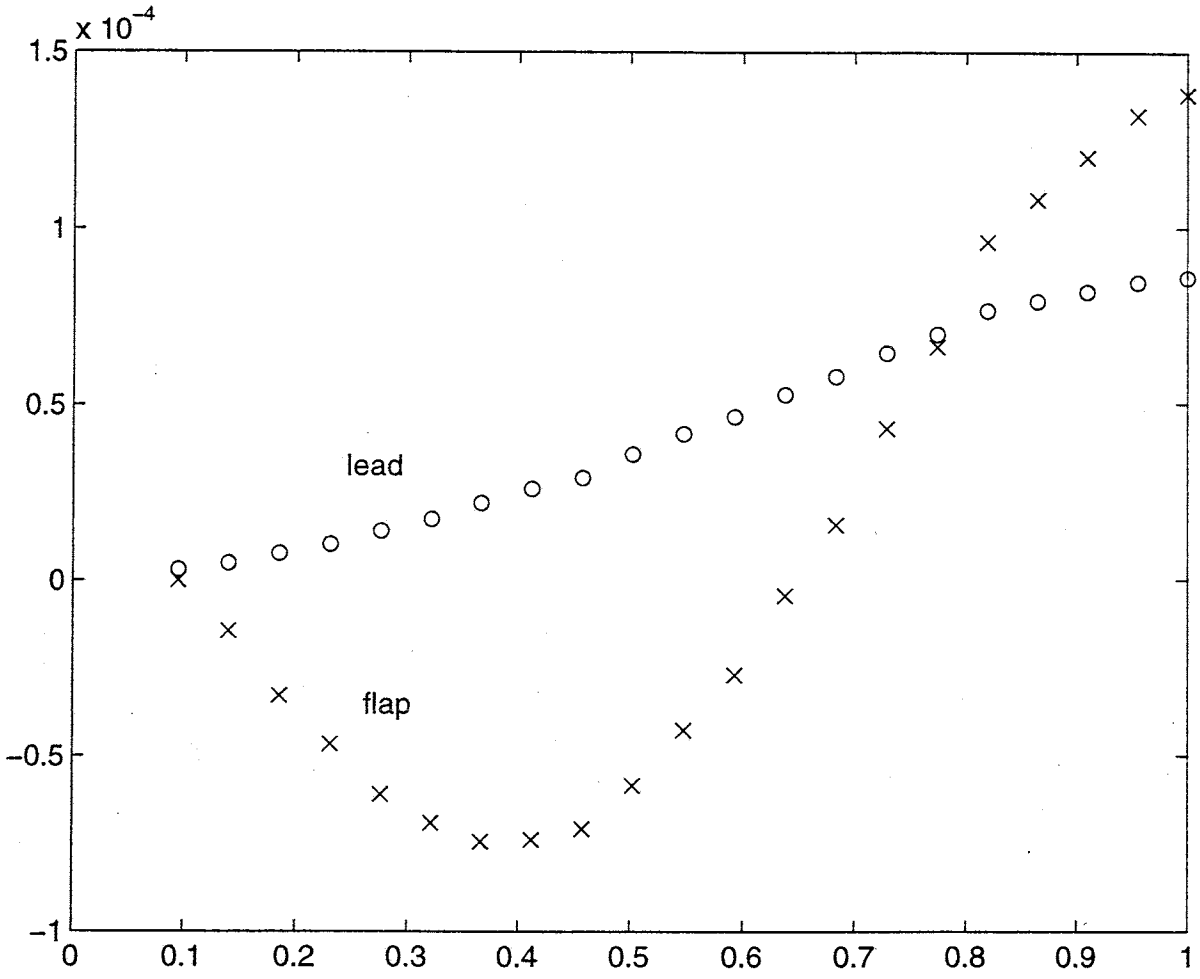

Figure 11 Lead-lag and flap displacements after 20 time steps of aeroelastic coupled motion (M(tip) = 0.296, collective = 4 degrees)